

An Analytical, Variable Resolution, Complete Description of Static Molecules and Their Intermolecular Binding Properties

Jr-Hung Lin and Timothy Clark*

Computer-Chemie-Centrum der Universitaet Erlangen-Nuernberg, Naegelsbachstrasse 25,
91052 Erlangen, Germany

Received February 16, 2005

A fully analytical description of molecular shape, as defined by the shrink-wrap isodensity or solvent-excluded surfaces and local properties related to Coulomb, donor/acceptor, and polarizability (dispersion) interactions is described. The molecular surface and four local properties adequate for describing intermolecular interactions (the molecular electrostatic potential and the local ionization energy, electron affinity, and polarizability) are fitted to spherical-harmonic expansions, which provide a compact and information-rich description of the properties of the static molecule. The resolution of the description can be varied from isotropic to near atomistic detail by adjusting the order of the individual spherical-harmonic expansions. Examples are given to illustrate the effect of truncating the different spherical-harmonic approximations.

INTRODUCTION

The essence of computer modeling in chemistry is the description of the molecules. Whereas quantum mechanical techniques describe atoms and molecules fairly realistically with the Born–Oppenheimer approximation, most fast simulation and modeling methods use multicenter atomistic descriptions whose major advantage is their ease of computation and programming. However, the assumption of isotropic atoms is inherent in most incarnations of these techniques (an exception, for instance, is the use of pseudo-atoms to represent lone pairs in some force fields).¹ Furthermore, there is no real justification of the atoms-in-molecules (AIM)² approach except that a given type of atom's electron density appears to be relatively transferable between similar molecules. We have therefore considered an alternative treatment for molecules in which only the molecular surface is considered.³ For a static molecule, this approach amounts to describing a three-dimensional object whose intermolecular binding properties are projected into local properties on its surface. With this aim, we have used the commonly used molecular electrostatic potential⁴ (labeled V in the following) and the local ionization energy (labeled I in the following) introduced by Sjöberg et al.⁵ and have extended the molecular description to include the local electron affinity⁶ (A) and the local polarizability⁶ (α). The local electron affinity is a simple extension of the concept of the local ionization energy, whereas the local polarizability is based on our parametrized version⁷ of Rivail's variational technique⁸ modified to allow us to calculate atomic and "orbital" polarizabilities within an additive model.⁹ These four properties have been shown³ to be able to treat intermolecular interactions accurately, to be a good basis for statistical surface-based descriptors for quantitative structure–property relationships (QSPR),¹⁰ and for surface-integral free-energy models.¹¹

Our model for describing molecules and their intermolecular interactions therefore consists of a molecular surface onto which the values of the four local properties are projected. This model is, however, purely numerical and requires $7n$ floating-point numbers storage, where n is the number of points used to define the surface, which is usually of the order of thousands for drug-sized molecules. We now report an analytical version of this molecular description whose resolution can be varied as required, allowing progressively finer searches in databases, for instance. This description can be expressed as a fixed-length vector of floating-point numbers for quantitative structure–activity relationships (QSAR) and QSPR. Our molecular description is based on spherical-harmonic expansions, which have been used previously by Max and Getzoff,¹² Olson et al.,¹³ and Ritchie and Kemp¹⁴ to treat proteins but as far as we are aware not for small molecules. The major advantage of spherical harmonics for high-throughput applications is that common operations such as rotation, superimposition, or docking can be performed very efficiently analytically.¹⁴

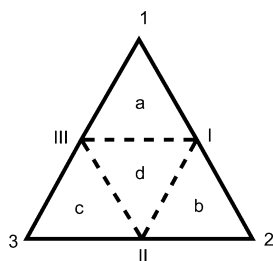
THEORY

All results reported here are based on AM1¹⁵ semiempirical molecular orbital (MO) calculations, although electron densities derived from any other technique could be used. For extensive basis-set *ab initio* or density functional theory (DFT) calculations, however, an alternative formulation of the local electron affinity⁶ would be needed because the large number of diffuse virtual orbitals would make the simple Koopmans approach almost meaningless. Alternatives derived from the local hardness are being investigated. All MO calculations used VAMP 9.0¹⁶ and surfaces, local properties, and spherical-harmonic fitting used ParaSurf 1.0.¹⁷

Molecular Shape. Molecular surfaces described by spherical harmonics must be single valued along any given radial vector from the center. We therefore generated the surfaces

* Corresponding author e-mail: clark@chemie.uni-erlangen.de.

to be fitted using a shrink-wrap algorithm.¹⁸ Shrink-wrap algorithms approach the center of the molecule along a radial vector to the center from a sphere outside the molecule. The first encounter with the molecule defines the shrink-wrap surface point along the relevant radial vector. Shrink-wrap surfaces are therefore single-valued along any radial direction from the center, a requirement for fitting to spherical-harmonic expansions. The surface was determined either as an isodensity surface¹⁹ at a density value of $0.0002 \text{ e}^- \text{ \AA}^{-3}$ or as a shrink-wrap version of a solvent-excluded surface.²⁰ To avoid hydrogens, which have little electron density, protruding through the fitted surface, the isodensity value was chosen to be slightly lower than usual, and the van der Waals' radius of hydrogen was set to 1.5 \AA . Standard values of van der Waals' radii were used for all other elements and a solvent-probe radius of 1.0 \AA . An initial spherical grid outside the bounds of the molecule was used to determine the initial points on the shrink-wrap surface, after which large triangles (in this work, area $> 0.3 \text{ \AA}^2$) were subdivided into four as shown below.



The original triangle, defined by the points 1, 2, and 3, is divided into four new ones, a–d, by creating the new corners I, II, and III at the midpoints (defined in terms of the Euler angles and the isodensity value, not the geometrical midpoint) of their respective sides of the original triangle. This procedure is not ideal for areas in which the shrink-wrap surface lies considerably outside the isodensity surface but performs adequately.

The radial distance, r , of the surface points from the molecular center (usually the center of gravity unless this is outside the molecule) is then fitted to a real spherical-harmonic expansion according to

$$r(\theta, \phi) = \sum_{l=0}^N \sum_{m=-l}^l a_{lm} y_{lm}(\theta, \phi) \quad (1)$$

where N is the order of the spherical-harmonic expansion used, a_{lm} are the fitting coefficients, and $y_{lm}(\theta, \phi)$ are real spherical harmonics given by

$$y_{lm}(\theta, \phi) = \{N_{lm} P_{lm}(\cos\theta) \cos|m|\phi, m \geq 0$$

and

$$y_{lm}(\theta, \phi) = \{N_{lm} P_{lm}(\cos\theta) \sin|m|\phi, m < 0 \quad (2)$$

where N_{lm} are normalization factors and $P_{lm}(\cos \theta)$ are associated Legendre functions.^{12,13} The fitting coefficients a_{lm} are given²² by

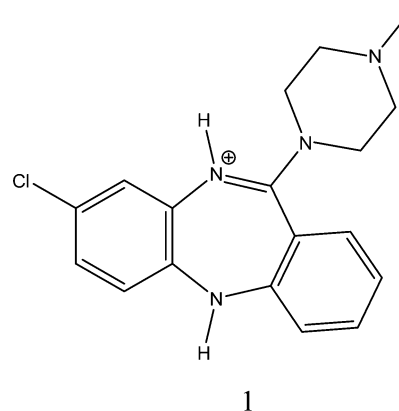
$$a_{lm} = \int_0^{2\pi} \int_0^\pi r(\theta, \phi) y_{lm}(\theta, \phi) \sin \theta d\theta d\phi \quad (3)$$

This fitting procedure has the advantage that the error decreases monotonically with increasing N , so that the spherical harmonic expansion can be fitted to an arbitrary degree of accuracy and, once fitted, can be truncated to any convenient degree $\leq N$.

Local Properties. Once the fitted surface has been determined according to eqs 1–3, the local properties can be determined at the surface points and expressed as functions of the Euler angles, θ and ϕ . These properties can, in turn be fitted to spherical-harmonic expansions to give a total of five such expansions describing the molecular shape as $r(\theta, \phi)$ and the four local properties $V(\theta, \phi)$, $I(\theta, \phi)$, $A(\theta, \phi)$, and $\alpha(\theta, \phi)$. This description of the molecule reduces to the five sets of coefficients a_{lm} or $5(N + 1)^2$ floating-point numbers.

RESULTS

Shape Fitting. Figure 1 shows the results obtained for protonated clozapin, **1**, using different orders for the spheri-



cal-harmonic fit and Figure 2 a plot of the root-mean-square (RMS) error in the fitted radii from the center as a function of the order of the spherical-harmonic fit. The RMS error decreases steeply below $l = 4$, where it attains a value of 0.45 \AA , and more slowly at higher values of l . The rate of improvement of the fit is very low at the highest value shown, $l = 15$, where the RMS error is 0.14 \AA . The center was in this case the center of mass, so that the only effect of increasing l from zero (a sphere) to one is to shift the center of the essentially spherical surface. This effect is exactly analogous to polarizing s -orbitals with p -functions in LCAO (linear combination of atomic orbitals) molecular orbital theory. The biggest improvements in the shape description are given by adding $l = 2, 3$, and 4 (corresponding to the angular part of d, f , and g orbitals, respectively, to give a familiar description of the spherical harmonics). The RMS error decreases from over 2.5 \AA for $l = 1$ to 0.45 for $l = 4$ and the visual impression of the fit improves dramatically (Figure 1). For many high-throughput but low-resolution applications, shape descriptions using $l = 4$ (25 coefficients) or 5 (36 coefficients) would be perfectly adequate.

Further increases in the order of the spherical-harmonic expansion result in detailed refinement of the surface but no obvious change in the overall shape. Spherical-harmonic shape coefficients can therefore provide efficient analytical descriptions of the shapes of small molecules, as has already been pointed out for proteins by Duncan and Olson¹³ and Kemp and Ritchie.¹⁴

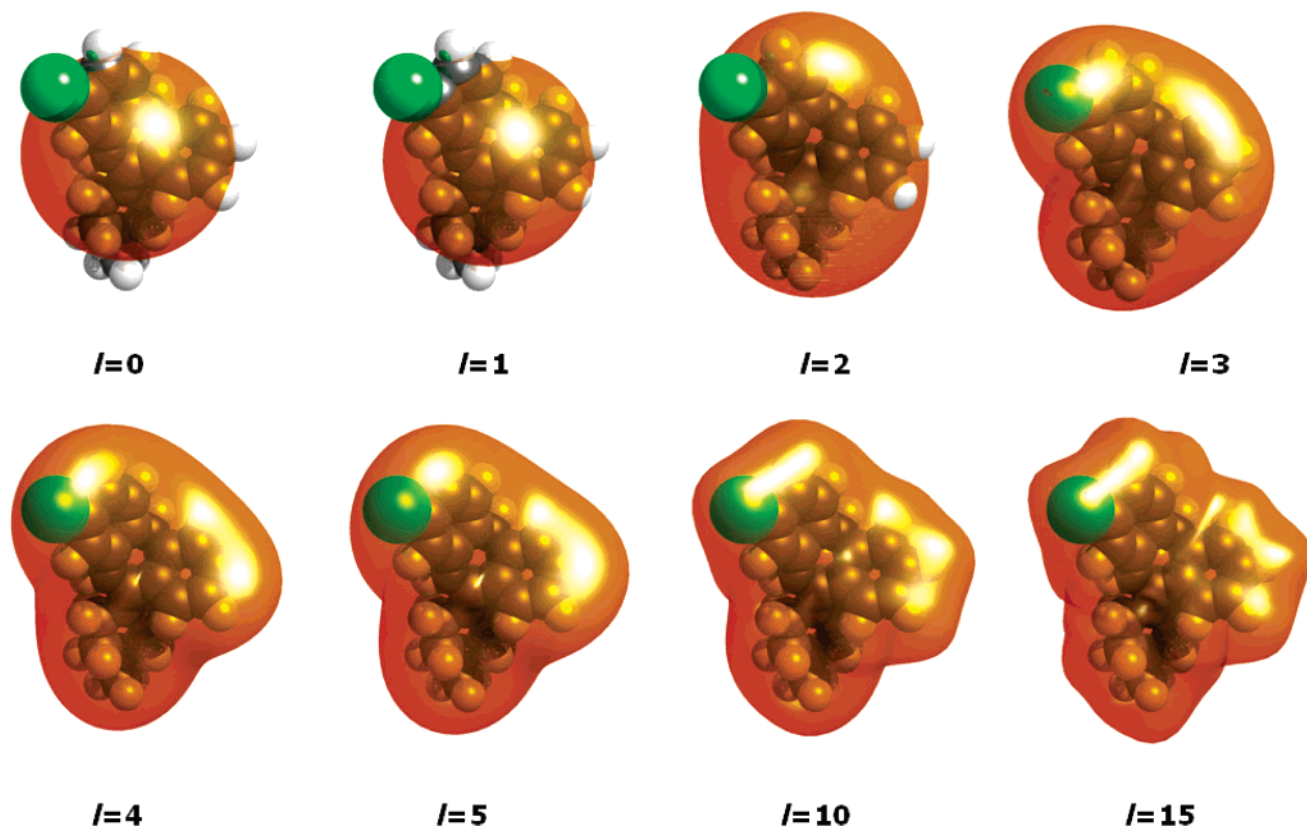


Figure 1. Spherical-harmonic fits of order l to the isodensity surface of clozapin. The molecule is shown as a CPK model (carbon gray, hydrogen white, nitrogen blue, and chlorine green) and the fitted surface in transparent orange.

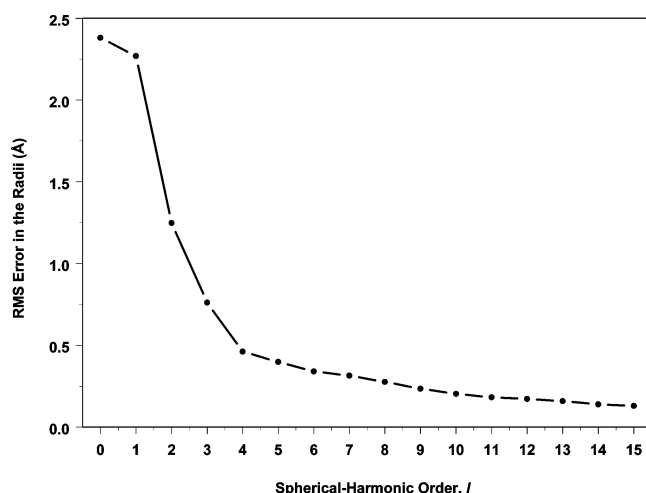


Figure 2. Dependence of the RMS error in the calculated radii on the order of the spherical-harmonic expansion for protonated clozapin. The RMS error is defined as the RMS difference between the shrink-wrap radii and those obtained from the spherical-harmonic fit.

Property Fitting. There is, however, no reason to describe only the molecular shape analytically in the above fashion. Intermolecular binding properties, expressed as the values of the four local properties described in the Introduction, at the molecular surface can also be described as additional spherical-harmonic expansions. Figure 3 shows the fits of the molecular electrostatic potential, V , for clozapin at the $l = 15$ spherical-harmonic surface shown in Figure 1. The color scale is the same for each value of l , so that the electrostatics can be compared directly. Figure 4 shows the

dependence of the RMS error in the fitted potentials as a function of l .

The results are similar to those for the shape fitting. The dipolar fit ($l = 1$, $\text{RMS} = 9.7 \text{ kcal mol}^{-1}$) is marginally worse than the $l = 0$ value ($9.3 \text{ kcal mol}^{-1}$) but adding quadrupole ($l = 2$, $\text{RMS} = 7.0$) contributions improves the overall fit significantly. By $l = 14$ the RMS error has fallen to 1 kcal mol^{-1} or 1.6% of the total range. However, the positive area of electrostatic potential associated with the protonated nitrogen does not become apparent until l is larger than 3, and the negative area adjacent to the chlorine is only between $l = 10$ and 15. There are, however, no significant changes for values of l larger than 10. Especially the relatively high order needed to describe the electrostatics of the chlorine substituent correctly suggests that relatively high orders for the spherical-harmonic expansion (between 10 and 15) are needed to describe specific binding features such as those typically used for pharmacophore²² or docking²³ techniques. Nevertheless, note that using $l = 6$ (49 coefficients) to describe the MEP of clozapin (43 atoms) requires roughly the same number of floating-point values as a simple atomic monopole model. Fitting atomic monopoles to the AM1 electrostatic potential²⁴ gives an RMS error for the MEP at the $l = 15$ surface of $23.0 \text{ kcal mol}^{-1}$ (mean signed and unsigned errors are 0.8 and $19.0 \text{ kcal mol}^{-1}$, respectively), compared with $3.2 \text{ kcal mol}^{-1}$ for the $l = 7$ spherical-harmonic fit. The atomic multipole model used to generate the electrostatics requires 243 atomic monopole, dipole and quadrupole components, corresponding roughly to the $l = 15$ spherical-harmonic expansion. However, the atomic-multipole technique also requires the Cartesian coordinates

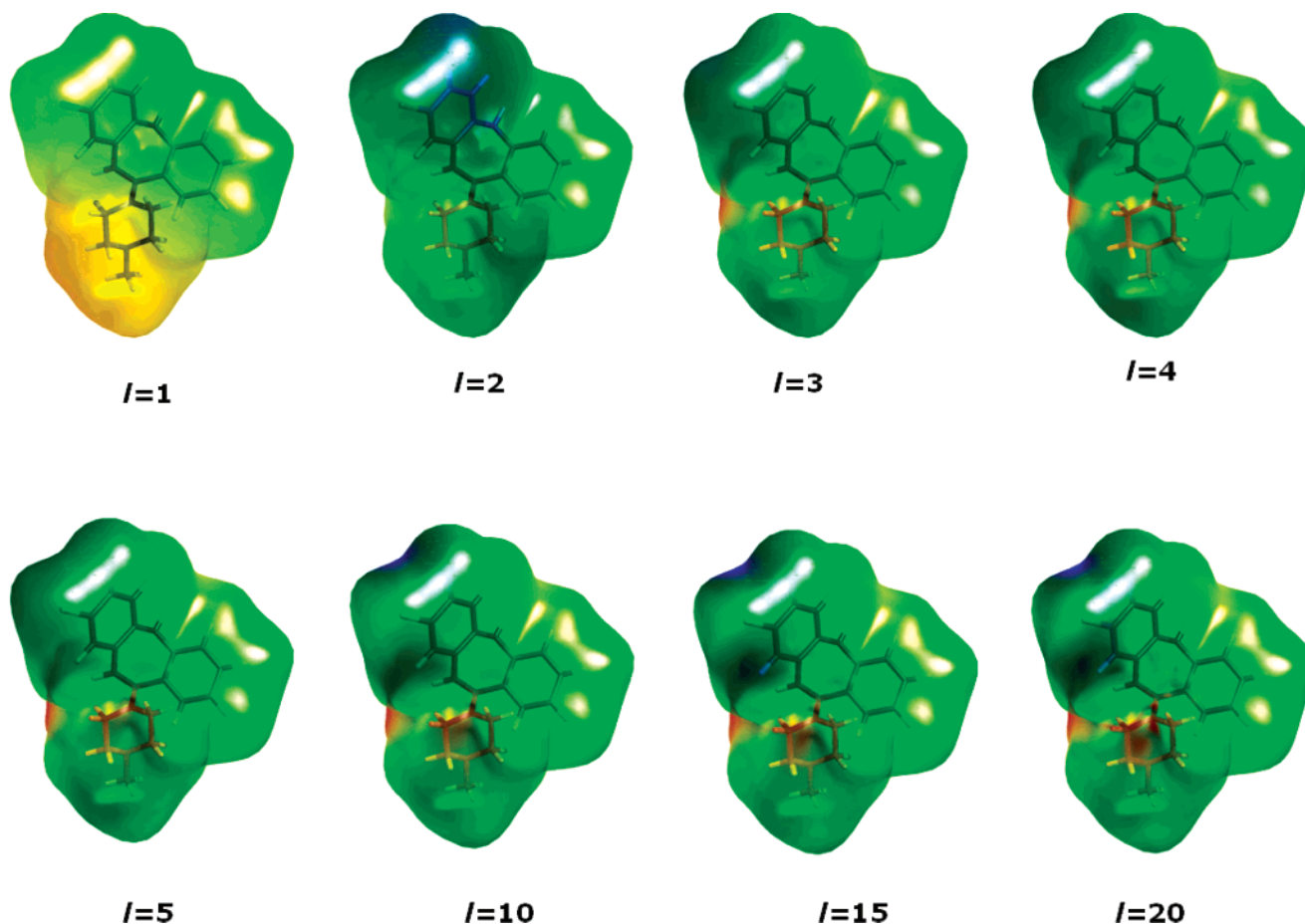


Figure 3. The molecular electrostatic potential (kcal mol^{-1} , blue = +31, red = +87) projected onto the $l = 15$ surface of protonated clozapin for different orders of the spherical-harmonic series for the MEP. The molecular framework is shown as a stocks model with the same atomic color coding as in Figure 1.

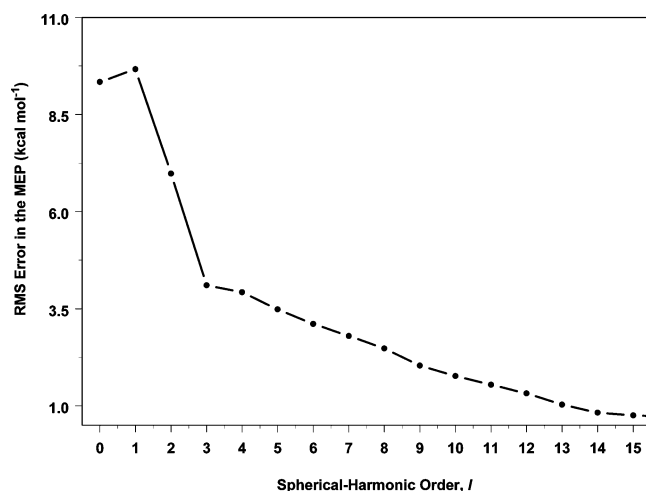


Figure 4. Dependence of the RMS error in the calculated MEP on the order of the spherical-harmonic expansion for clozapin.

of the atoms, giving a total of 372 floating-point values or roughly the equivalent of $l = 18$.

In the case of the MEP, the spherical-harmonic approach is closely related to a single-center multipole expansion for the molecular electrostatics.²⁵ In some cases, such multipole expansions do not converge but rather oscillate. This problem might also be anticipated for the approach outlined here. However, the inadequacies of the shrink-wrap surface are very similar to the causes of oscillation in monocentric multipole fits, so that nonconvergence of the property fits

should not be a problem. Eventually, the fit becomes finer than the triangulation used to construct the spherical-harmonic fit, in which case the RMS-deviation can become larger. The goodness of fit is therefore a function of the graining of the fitted surface. Note also, as will be shown below, that much information to the biological activity of molecules is contained in the higher terms, whereas the lower terms probably are most relevant for modeling physical properties.

The other local properties can be fit in exactly the same way and will not be described here. However, Figure 5 shows the convergence of the fits for the shape and the four local properties expressed as percentages of the total range of the property for clozapin. As can be seen, the fits converge as expected, and all four properties can be described accurately and parsimoniously by individual spherical-harmonic expansions.

Spherical-Harmonic Coefficients as QSAR Descriptors.

The five individual spherical-harmonic expansions (shape, V , I , A , and α) provide a complete description of the molecule and its intermolecular binding properties. Thus, the coefficients of these expansions, a_{lm}^r , a_{lm}^V , a_{lm}^I , a_{lm}^A , and a_{lm}^α , respectively, are also candidates as descriptors for quantitative structure–activity relationships (QSARs). To test this hypothesis, we have used the overlaid structures of 25 dopamine-D4 antagonists taken from an earlier CoMFA²⁷ study.²⁸ Note that our purpose here is not to introduce a new QSAR technique but rather to test the information content

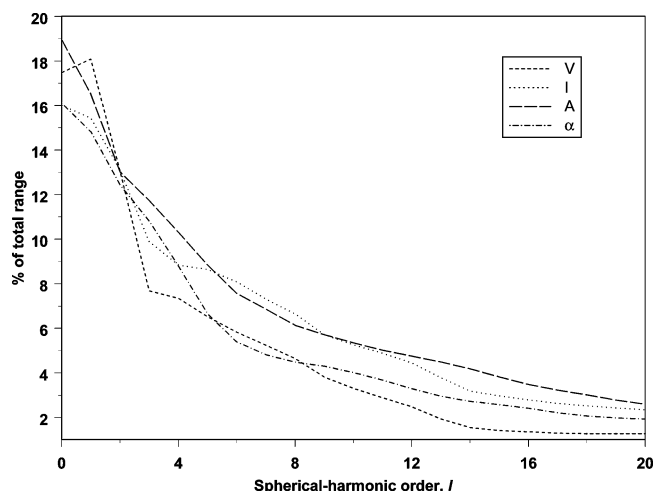


Figure 5. RMS errors in % of the maximum RMS for the shape and the four local properties. The RMS errors at $l = 15$ are 0.14 Å, 0.98 kcal mol⁻¹, 0.63 and 0.21 eV and, 0.008 Å³ for shape, V, I, A, and α , respectively.

and the usefulness of the coefficients as descriptors for a data set for which the performance of CoMFA has been established. We therefore used exactly the same overlaid structures as were used for the CoMFA study and performed single-point AM1 calculations to obtain the spherical-harmonic coefficients. These were subjected to stepwise multiple linear regression using the forward and backward stepping algorithm implemented in TSAR²⁹ with the number of steps set to four to give a four-term model. Models with larger numbers of terms (up to six) did not have significantly better r_{cv}^2 values than that reported in eq 4. Further work has shown that the model obtained is extremely robust and does not vary when a variety of alternative multivariate regression techniques are used. Thus, the choice of regression technique is not important.

As might be expected, the shape and MEP coefficients played the major role in the regression equations obtained, so that we limited our model to these two types of coefficients. The a_{lm}^r and a_{lm}^v values up to $l = 15$ (a total of 512 coefficients per molecule) were used as potential descriptors. This procedure resulted in a model with four descriptors given in eq 4:

$$pK_i = 3.132(\pm 0.311)a_{4,4}^r - 8.975(\pm 1.759)a_{9,-1}^r + 14.745(\pm 3.267)a_{13,-9}^r + 0.788(\pm 0.206)a_{11,-11}^v + 6.144(\pm 0.172) \quad (4)$$

$$N = 25, r^2 = 0.896, r_{cv}^2 = 0.753,$$

$$f\text{-probability} = 1.3 \times 10^{-10}$$

The cross-validated r^2 -value refers to a leave-one-out procedure. The coefficients of the four descriptors (in the order given in eq 4) using standardized data are 1.012, -0.514, 0.461, and 0.378, so that the model is well balanced with significant contributions from all four descriptors. Analogous regression analyses on all 512 descriptors with randomized pK_i -values gave $r^2 = 0.721$ and $r_{cv}^2 = -2.330$. For comparison, the CoMFA study using the same pK_i -data used seven terms plus the constant in the final equation (obtained from a total of 8280 grid points) and gave a cross-validated r^2 of

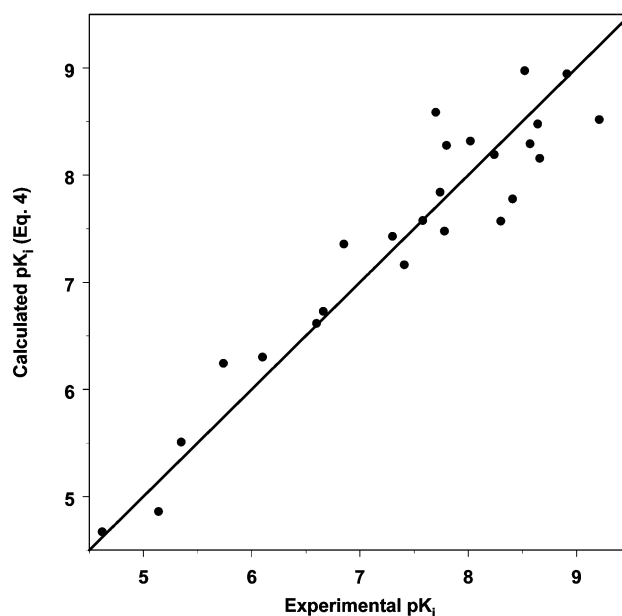


Figure 6. Comparison of the experimental and calculated (eq 4) pK_i values for the D4-antagonist data set from ref 28. The line is the 1:1 corresponding not the best-fit. The standard error is 0.443 log units.

0.784. The results obtained from eq 4 are shown graphically in Figure 6. Thus, this direct comparison suggests that the coefficients of the spherical-harmonic expansions for the molecular shape and electrostatics are at least as useful descriptors as probe energies obtained at grid points in a CoMFA analysis. Note that, although the remaining local properties do not play a role in determining the biological activity in this example, they are extremely important for conventional QSPR models¹⁰ and in models derived from the integration of functions of the local surface properties.¹¹ Thus, a complete description of the molecular properties for QSAR may only require the shape and MEP but more exact QSPR models need the other local properties.

DISCUSSION

Our intention in this work was to define a purely analytical molecular description that is as parsimonious as possible and that offers the possibility of varying the resolution of the description as demanded by the application. We plan to use the molecular description introduced here for a variety of applications ranging from very high-throughput screening to high-quality model building. However, even at this early stage several important characteristics of the molecular description are clear.

The comparison with the CoMFA study reported in ref 28 demonstrates that the essential information for QSAR models is contained in the shape and MEP-coefficients. The technique used to build the model reported in eq 4 is not yet practicable because it relies on a prealigned data set, in this case using the same alignment as used for the CoMFA study. Clearly, up to a rotation, the descriptions are orientation-independent, but superimpositions can easily be achieved by using the rotational properties of the spherical harmonic expansion coefficients.^{13,14} Our results suggest that spherical-harmonic expansions up to roughly $l = 10$ –12 should be adequate for most quantitative applications. We envision a series of applications from QSAR at varying resolutions

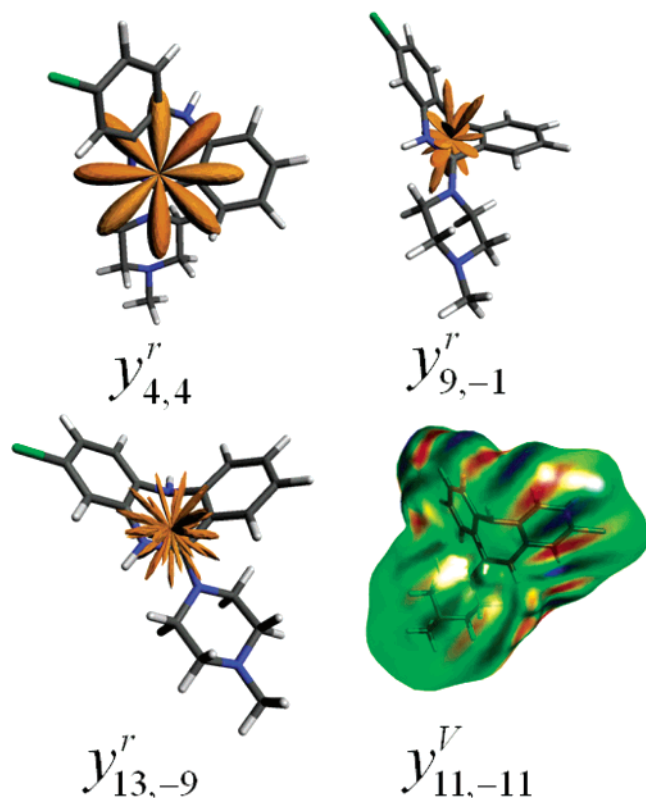


Figure 7. The shape (left) and electrostatic potential (right) components of the spherical-harmonic expansions that contribute to the QSAR (eq 4).

using either similarity or docking approaches. Steadily increasing the resolution of the molecular description promises to be an excellent approach to screening very large data sets efficiently.

The model introduced here is, however, not only applicable to QSAR and QSPR. We are currently constructing a water model for molecular dynamics or Monte Carlo simulations that describes the fixed-geometry water molecules as spherical-harmonic shape, MEP, donor–acceptor, and dispersion expansions. The advantage of such a model is that it can easily be made polarizable by varying the coefficients in the spherical-harmonic expansion for the MEP.

The major disadvantage of this approach is that the results are difficult to interpret. Take, for instance the QSAR reported in eq 4. Figure 7 shows the shape and MEP-distributions represented by the four coefficients that appear in the equation. They convey little or no understandable information about what promotes or decreases activity and thus reduce the technique to a pure search tool, rather than an aid to design. Clearly, new interpretive tools will be needed to address this issue.

However, a potentially important feature of the molecular description presented here is that it does not contain the molecular structure, so that, at low enough resolution, it represents a potential way of communicating molecular properties without the structure.

ACKNOWLEDGMENT

We thank the Deutsche Forschungsgemeinschaft for financial support and David Ritchie, Martyn Ford, Jonathan Essex, and Brian Hudson for many fruitful discussions. We

also thank Harry Lanig for providing us with the overlaid structures of the D4-antagonist data set from ref 28.

REFERENCES AND NOTES

- (1) See, for instance, Waldman, M.; Masek, B. B. Analytical energy derivatives and normal modes in force fields employing lone-pair pseudo atoms. *J. Comput. Chem.* **1989**, *10*, 856–60.
- (2) Bader, R. F. W. *Atoms in Molecules: A Quantum Theory*; Oxford University Press: Oxford, 1994.
- (3) Clark, T. QSAR and QSPR based solely on surface properties? *J. Mol. Graph. Model.* **2004**, *22*, 519–525.
- (4) Murray, J. S.; Politzer, P. Statistical Analysis of the Molecular Surface Electrostatic Potential: An Approach to Describing Noncovalent Interaction in Condensed Phases. *J. Mol. Struct. (THEOCHEM)* **1998**, *425*, 107–114. Murray, J. S.; Lane, P.; Brinck, T.; Paulsen, K.; Grince, M. E.; Politzer, P. Relationships of Critical Constants and Boiling Points to Computed Molecular Surface Properties. *J. Phys. Chem.* **1993**, *97*, 9369–9373.
- (5) Sjöberg, P.; Murray, J. S.; Brinck, T.; Politzer, P. A. Average local ionization energies on the molecular surfaces of aromatic systems as guides to chemical reactivity. *Can. J. Chem.* **1990**, *68*, 1440–1443.
- (6) Ehresmann, B.; Martin, B.; Horn, A. H. C.; Clark, T. Local molecular properties and their use in predicting reactivity. *J. Mol. Model.* **2003**, *9*, 342–347.
- (7) Schürer, G.; Gedeck, P.; Gottschalk, M.; Clark, T. Accurate Parametrized Variational Calculations of the Molecular Electronic Polarizability by NDDO–Based Methods. *Int. J. Quantum Chem.* **1999**, *75*, 17–31.
- (8) Rinaldi, D.; Rivail, J. L. Calculation of molecular electronic polarizabilities. Comparison of different methods. *Theor. Chim. Acta* **1974**, *32*, 243–251. Rinaldi, D.; Rivail, J. L. Molecular polarisability and dielectric effect of medium in the liquid phase. Theoretical study of the water molecule and its dimers. *Theor. Chim. Acta* **1973**, *32*, 57–70.
- (9) Martin, B.; Gedeck, P.; Clark, T. An Additive NDDO–Based Atomic Polarizability Model. *Int. J. Quantum Chem.* **2000**, *77*, 473–497.
- (10) Ehresmann, B.; de Groot, M. J.; Clark, T. New Molecular Descriptors Based on Local Properties at the Molecular Surface and a Boiling-Point Model Derived from Them. *J. Chem. Inf. Comput. Sci.* **2004**, *43*, 658–668.
- (11) Ehresmann, B.; de Groot, M. J.; Clark, T. Surface-Integral QSPR Models: Local Energy Properties. *J. Chem. Inf. Model.*, in press.
- (12) Max, N. L.; Getzoff, E. D. Spherical Harmonic Molecular Surfaces. *IEEE Comput. Graphics Appl.* **1988**, *8*, 42–50.
- (13) Duncan, B. S.; Olson, A. J. *Approximation and Characterization of Molecular Surfaces*; Scripps Institute: San Diego, California, 1995.
- (14) Ritchie, D. W.; Kemp, G. J. L. Fast computation, rotation, and comparison of low resolution spherical harmonic molecular surfaces. *J. Comput. Chem.* **1999**, *20*, 383–395. Ritchie, D. W. Parametric Protein Shape Recognition, Ph.D. Thesis, University of Aberdeen, 1998 (http://www.csd.abdn.ac.uk/~dritch/papers/ritchie_thesis.pdf).
- (15) Dewar, M. J. S.; Zebisch, E. G.; Healy, E. F.; Stewart J. J. P. The development and use of quantum mechanical molecular models. 76. AM1: a new general purpose quantum mechanical molecular model. *J. Am. Chem. Soc.* **1985**, *107*, 3902–3909. Holder, A. J. *AM1, Encyclopedia of Computational Chemistry*; Schleyer, P. v. R., Allinger, N. L., Clark, T., Gasteiger, J., Kollman, P. A., Schaefer, H. F., III., Schreiner, P. R., Eds.; Wiley: Chichester, 1998; pp 8–11.
- (16) Clark, T.; Alex, A.; Beck, B.; Burkhardt, F.; Chandrasekhar, J.; Gedeck, P.; Horn, A. H. C.; Hutter, M.; Martin, B.; Rauhut, G.; Sauer, W.; Schindler, T.; Steinke, T. *VAMP 9.0*, Erlangen, 2005.
- (17) Clark, T.; Lin, J.-H.; Horn, A. H. C. ParaSurf 1.0, Computer-Chemie-Centrum, University of Erlangen, Erlangen, 2004/5.
- (18) Cai, W.; Zhang, M.; Maigret, B. New approach for representation of molecular surface. *J. Comput. Chem.* **1998**, *19*, 1805–1815.
- (19) Loew, L. M.; MacArthur, W. R. A molecular orbital study of monomeric metaphosphate. Density surfaces of frontier orbitals as a tool in assessing reactivity. *J. Am. Chem. Soc.* **1977**, *99*, 1019–25.
- (20) Sanner, M. F.; Olson, A. J.; Spehner, J. C. Reduced surface: an efficient way to compute molecular surfaces. *Biopolymers* **1996**, *38*, 305–20.
- (21) Lanczos, C. *Discourse on Fourier Series*; Oliver and Boyd: London, 1966.
- (22) See, for instance, Guner, O. F. History and evolution of the pharmacophore concept in computer-aided drug design. *Curr. Top. Med. Chem.* **2002**, *2*, 1321–1332.

- (23) See, for instance, Kitchen, D. B.; Decornez, H.; Furr, J. R.; Bajorath, J. Docking and scoring in virtual screening for drug discovery: methods and applications. *Nature Rev. Drug Disc.* **2004**, *3*, 935–949.
- (24) Beck, B.; Clark, T.; Glen, R. C. A Detailed Study of VESPA Electrostatic Potential-Derived Atomic Charges. *J. Mol. Model.* **1995**, *1*, 176–187.
- (25) Horn, A. H. C.; Lin, J.-H.; Clark, T. Multipole electrostatic model for MNDO-like techniques with minimal valence *spd*-basis sets. *Theor. Chem. Acc.* **2005**, *113*, in press.
- (26) Stone, A. J. *The Theory of Intermolecular Forces*; Clarendon Press: Oxford, 2002.
- (27) Cramer, R. D., III.; Patterson, D. E.; Bunce, J. D. Comparative molecular field analysis (CoMFA). 1. Effect of shape on binding of steroids to carrier proteins. *J. Am. Chem. Soc.* **1988**, *110*, 5959–67.
- (28) Lanig, H.; Utz, W.; Gmeiner, P. Comparative Molecular Field Analysis of Dopamine D4 Receptor Antagonists Including 3-[4-(4-Chlorophenyl)piperazin-1-ylmethyl]pyrazolo[1,5-a]pyridine (FAUC 113), 3-[4-(4-Chlorophenyl)piperazin-1-ylmethyl]-1H-pyrrolo[2,3-b]pyridine (L-745, 870), and Clozapin. *J. Med. Chem.* **2001**, *44*, 1151–1157.
- (29) TSAR 3.3, Oxford Molecular PLC, Oxford, 2000.

CI050059V